A TEORELL OSCILLATOR SYSTEM WITH FINE PORE MEMBRANES

P. LANGER, K. R. PAGE, AND G. WIEDNER, *Max-Planck-Institut für Biophysik, 6000 Frankfurt 70, Federal Republic of Germany and Biophysical Chemistry Unit, Department of Chemistry, University of Aberdeen, Aberdeen, Scotland*

ABSTRACT A Teorell membrane oscillator system has been investigated theoretically and experimentally. Instead of the broad pore (e.g., glass sinter) membranes used by Teorell and other investigators, we used membranes of a hydrodynamic permeability lower by a factor of 10^3–10^5 and a fixed ion concentration higher by a factor of 10^2–10^5. A system with such membranes was thought to be a more adequate analogue of excitable biological tissues (for which the Teorell oscillator had been presented as a model). Stationary state voltage-current curves were recorded, and flip-flops were only found in membranes whose hydrodynamic permeability was above a certain value. A theoretical description, agreeing closely with the experimental findings, is given in terms of the Nernst-Planck-Schlögl equations; flip-flops are predicted only if the hydrodynamic permeability is above and the fixed ion concentration is below a critical value. These values depend on the hydrostatic pressure and on the ratio of the cation and anion diffusion coefficient in the membrane, and they are found to be far beyond (~3 orders of magnitude) the data for membranes used by others in similar experiments. Although our theoretical analysis demonstrates that the Teorell mechanism is ineligible as a source of excitability in those biological systems for which sufficient data are available to permit comparison, the membrane properties for which the theory predicts flip-flops are such that it cannot be excluded a priori.

INTRODUCTION

The Teorell membrane oscillator is an electrochemical system that shows an oscillatory response to electrical or mechanical stimuli that is similar to what can be observed in excitable tissues such as nerve or muscle cells or cells of certain giant algae. It was first studied by Teorell, who employed glass sinter, porcelain, or ion exchange gel membranes (Teorell, 1956, 1959*a*, 1959*b*, 1961*a*). Franck (1963, 1967) and Drouin (1969*a*, *b*) used quartz powder membranes; Meares and Page (1972, 1973, 1974; Page and Meares, 1974) studied Nuclepore membranes, which have pores of very well defined shape and size.

As detailed analysis of the oscillation phenomena has been given by Franck (1963) and by Page and Meares (1974), we shall limit ourselves here to recalling briefly some important points. The Teorell oscillator system is shown schematically in Fig. 1. A porous membrane of low internal charge separates two well stirred electrolyte solutions of different concentrations. There are two counteracting driving forces in the system: one is the electric potential difference across the membrane, owing to a constant electric current, which generates an electroosmotic volume flow through the membrane; and the other is the hydrostatic pressure difference that arises from the difference of the levels of the solution in each compartment and causes a volume flow in the opposite direction. Both forces depend on the net volume flow,

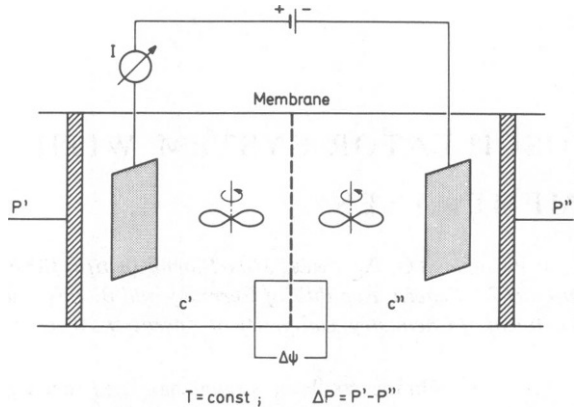

FIGURE 1 Schematic representation of the Teorell oscillator system.

because this flow is responsible for filling the membrane either with concentrated or with dilute solution (Fig. 2), which produces different electric potential drops (I = constant), and for shifting the solution levels in the compartments, which causes different hydrostatic pressures. Thus, oscillations of the electric potential, the hydrostatic pressure, and the volume flow can be observed.

If in addition to the electric current the hydrostatic pressure difference is kept constant, the volume flow and therefore the membrane potential are completely determined, i.e., the system is stationary. Depending on the level at which current and pressure have been fixed, the membrane is either in a state of low or of high electric conductivity (Fig. 2). If the magnitude of the electric current is now altered by a sufficient amount, a transition from one state to the other occurs. Changing the electric current stepwise from low to higher values and back again, i.e., performing a sequence of galvanostatic measurements, leads to a curve as the one shown in Fig. 3*A*. The dotted lines represent the transitions (called "flip" and "flop") between the low and the high conductivity states during which no stationary states are possible. If instead of galvanostatic experiments potentiostatic measurements are made (i.e., the membrane potential and the pressure difference are kept constant), the resulting voltage-current curves have a shape such as is shown in Fig. 3*B*, the relative minimum and maximum corresponding to the current densities where the transitions occur in the galvanostatic case. Such nonmonotonic curves are characteristic of systems capable of oscillations.

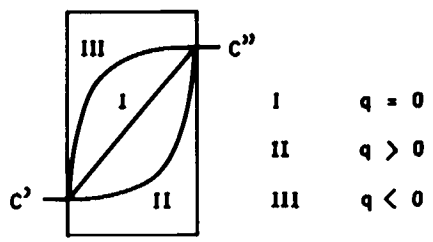

FIGURE 2 Concentration profile in a membrane of low fixed ion concentration dependent on the volume flow through the membrane.

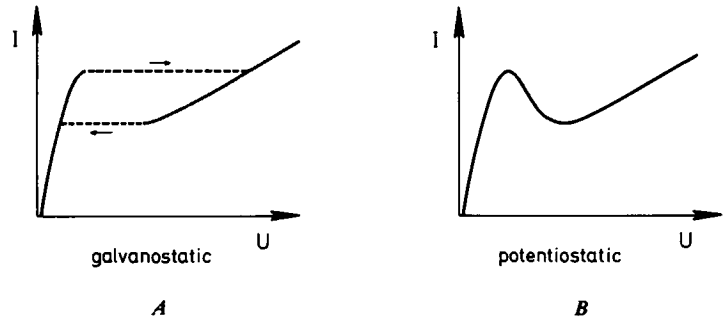

FIGURE 3 Stationary-state voltage-current curves showing a flip-flop transition between two states of different electric conductivity.

The oscillatory as well as the stationary state behavior of the Teorell oscillator bears a remarkable resemblence to excitation phenomena observed in biological systems. Teorell was able to describe the excitability of *Nitella* (giant algae) cells in terms of the theory developed for his artificial oscillator system and on the basis of these observations suggested that the underlying mechanisms might be essentially identical (Teorell 1958, 1961*b*). His calculations were, however, based on assumptions about certain theoretical parameters and not on membrane properties measured in independent experiments. Thus, a comparison of, e.g., the fixed ion concentration and the hydrodynamic permeability of *Nitella* cell walls with the corresponding data of the "traditional" Teorell oscillator membranes reveals a discrepancy of some orders of magnitude (see Table I). Generally, the hydrodynamic permeabilities of the former are found to be much lower than those of the membranes used in the Teorell oscillator, whereas the fixed ion concentrations are much higher. As these parameters, in Teorell's model, govern the oscillatory behavior of membranes, it seems worthwhile to examine an artificial membrane oscillator system containing a membrane with a fixed charge higher and a hydrodynamic permeability lower than studied before.

In this paper we shall present results from experiments with synthetic membranes of pore sizes of 40–1,000 Å; their stationary state flip-flop behavior has been studied instead of oscillations because the periods would become very long (the pressures required—up to ~3 bars—cannot be built up by the small volume flows in a reasonable amount of time). We shall also present an appropriate theoretical analysis that is valid for membranes of high fixed ion concentrations and small pore diameters, and we shall show how this theory might serve to determine in an approximative fashion whether, in principle, the excitability of a specific biological membrane can be described by the Teorell mechanism.

THEORY

Flux Equations

For a discussion of transport in charged fine pore membranes with pore diameters in the order of 100 Å, one can imagine the counterions as being distributed homogeneously over the pore volume. This is the model of a fine pore membrane introduced by Schmid (1950, 1951, 1952; Schmid and Schwarz, 1951, 1952). On the basis of this model the Nernst-Planck-Schlögl equations (Schlögl, 1955, 1966; Schlögl and Schödel, 1956) will be used, which in addition to

diffusion and electric transference take into account a convective transport of ions through the membrane.

Because these equations are nonlinear and can be integrated in closed form only for the case of a binary electrolyte or for the bi-ionic case, only these cases shall be considered here; i.e., we have the following set of equations:

$$\Phi_1 = C_1 v - D_1 \frac{dC_1}{dx} - D_1 z_1 C_1 \frac{d\bar{\psi}}{dx}, \tag{1}$$

$$\Phi_2 = C_2 v - D_2 \frac{dC_2}{dx} - D_2 z_2 C_2 \frac{d\bar{\psi}}{dx}, \tag{2}$$

$$v = d_h \left(RT\omega X \frac{d\bar{\psi}}{dx} - \frac{d\bar{P}}{dx} \right). \tag{3}$$

The following symbols will be used:

c_i concentration of ion species i in solution phase
C_i concentration of ion i in membrane phase
z_i valency of ion species i
D_i diffusion coefficient of ion species i
Φ_i flux density of ion species i
I electric current density
v volume flux density
ω sign of fixed charges in the membrane (± 1)
X fixed ion concentration in the membrane
d_h hydrodynamic permeability of the membrane
$\bar{\phi}$ electric potential inside the membrane
$\bar{\psi}$ $= F/RT \cdot \bar{\phi}$ dimensionless electric potential inside the membrane
$\bar{P}$ pressure difference inside the membrane
R gas constant
T absolute temperature
F Faraday's constant.

The condition for electroneutrality in the membrane holds:

$$\sum_{i=1}^{2} z_i C_i + \omega X = 0. \tag{4}$$

It is now convenient to introduce two parameters (Schlögl, 1955) r and s instead of Φ_1 and Φ_2 through the following equations:

$$\Phi_1 = \frac{v\omega X}{4} \cdot \frac{z_1 D_1 - z_2 D_2}{z_1 z_2 D_2} (\omega - r)(\omega - s), \tag{5}$$

$$\Phi_2 = -\frac{v\omega X}{4} \cdot \frac{z_1 D_1 - z_2 D_2}{z_1 z_2 D_1} (\omega + r)(\omega + s). \tag{6}$$

Substituting these equations into Eqs. 1 and 2 we find

$$-\frac{1}{z_1D_1}(C+1)v+\frac{1}{z_1}\cdot\frac{dC}{dx}+(C+1)\frac{d\bar{\psi}}{dx}=\frac{v}{2}\cdot\frac{z_1D_1-z_2D_2}{z_1z_2D_1D_2}(\omega-r)(\omega-s), \tag{7}$$

$$-\frac{1}{z_2D_2}(C-1)v+\frac{1}{z_2}\cdot\frac{dC}{dx}+(C-1)\frac{d\bar{\psi}}{dx}=\frac{v}{2}\cdot\frac{z_1D_1-z_2D_2}{z_1z_2D_1D_2}(\omega+r)(\omega+s), \tag{8}$$

where the dimensionless variable

$$C=\frac{z_2C_2-z_1C_1}{\omega X}$$

has been introduced. Multiplying Eqs. 7 and 8 by $(C-1)$ and $(C+1)$, respectively, and subtracting the second equation from the first one yields

$$\frac{dC}{dx}=v\left(\frac{z_2}{D_1}-\frac{z_1}{D_2}\right)\frac{(C+\omega r)(C+\omega s)}{(z_2-z_1)C-(z_1+z_2)}, \tag{9}$$

while division of Eqs. 7 and 8 by z_2 and z_1, respectively, yields

$$\frac{d\bar{\psi}}{dx}=\frac{v\left[\frac{1}{2}\left(\frac{z_2}{D_1}-\frac{z_1}{D_2}\right)\frac{(1+\omega r)(1+\omega s)z_2-(1-\omega r)(1-\omega s)z_1}{z_1z_2}+\frac{C(D_2-D_1)+(D_1+D_2)}{D_1D_2}\right]}{(z_1-z_2)C+(z_1+z_2)} \tag{10}$$

Dividing Eq. 10 by Eq. 9 we obtain

$$\frac{d\bar{\psi}}{dC}=\left[\frac{(1-\omega r)(1-\omega s)z_1-(1+\omega r)(1+\omega s)z_2}{2z_1z_2}+\frac{C(D_2-D_1)+(D_1+D_2)}{z_1D_1-z_2D_2}\right]\Big/[(C+\omega r)(C+\omega s)]. \tag{11}$$

Eqs. 9 and 11 can now be integrated between the limits $x=0$ and $x=\delta$, $C=C'$ and $C=C''$, and $\bar{\psi}=0$ and $\bar{\psi}=-\Delta\bar{\psi}$:

$$v\left(\frac{z_2}{D_1}-\frac{z_1}{D_2}\right)\cdot\delta=\frac{(z_2-z_1)s+(z_1+z_2)\omega}{s-r}\ln\frac{C''+\omega s}{C'+\omega s}-\frac{(z_2-z_1)r+(z_1+z_2)\omega}{s-r}\ln\frac{C''+\omega r}{C'+\omega r}, \tag{12}$$

and

$$-\Delta\bar{\psi}=\frac{\omega}{s-r}\left[(A+\omega rB)\ln\frac{C''+\omega r}{C'+\omega r}-(A+\omega sB)\ln\frac{C''+\omega s}{C'+\omega s}\right], \tag{13}$$

where

$$A = \frac{(1 - \omega r)(1 - \omega s)z_1 - (1 + \omega r)(1 + \omega s)z_2}{2z_1z_2} + \frac{D_1 + D_2}{z_1D_1 - z_2D_2},$$

$$B = \frac{D_2 - D_1}{z_1D_1 - z_2D_2}.$$

Eq. 3 can be integrated directly to give

$$v\int_0^\delta dx = d_h\left(RT\omega X\int_0^{-\Delta\bar{\psi}} d\psi - \int_{P'}^{P''} d\bar{P}\right),$$

$$v = \frac{d_h}{\delta}(\Delta\bar{P} - RT\omega X\Delta\bar{\psi}), \tag{14}$$

where $\Delta\bar{P} = \bar{P}' - \bar{P}''$. Using this equation to eliminate v from Eqs. 12 and 13, we have two transcendental equations for the two variables r and s. For numerical computation of voltage-current relations a value for $\Delta\bar{\psi}$ is put into Eqs. 12 and 13, and the parameters r and s are evaluated by numerical methods normally applied to transcendental equations. When these parameters are substituted in Eqs. 5 and 6 to obtain the ion fluxes Φ_1 and Φ_2, the current density follows from the definition

$$I = F \cdot \sum_{i=1}^{2} z_i\Phi_i. \tag{15}$$

Repeating this procedure for every desired value of $\Delta\bar{\psi}$ yields a voltage-current curve. Often, however, there is a certain range of $\Delta\bar{\psi}$ for which real roots r and s cannot be obtained. In this case, complex roots can be evaluated by writing $r = x + iy$ and $s = x - iy$ (r and s have to be complex conjugates to keep the ion fluxes real). Then Eqs. 5 and 6 have the form

$$\Phi_1 = \frac{v\omega X}{4} \cdot \frac{z_1D_1 - z_2D_2}{z_1z_2D_2}[(\omega - x)^2 + y^2], \tag{16}$$

$$\Phi_2 = -\frac{v\omega X}{4} \cdot \frac{z_1D_1 - z_2D_2}{z_1z_2D_1}[(\omega + x)^2 + y^2]. \tag{17}$$

Proceeding as above for real r and s we obtain after integration

$$v\left(\frac{z_2}{D_1} - \frac{z_1}{D_2}\right)\delta = \frac{(z_2 - z_1)}{2}\ln\left[\frac{(C'' + \omega x)^2 + y^2}{(C' + \omega x)^2 + y^2}\right] - \frac{(z_2 - z_1)\omega x + (z_1 + z_2)}{y}\left(\operatorname{arctg}\frac{C'' + \omega x}{y} - \operatorname{arctg}\frac{C' + \omega x}{y}\right) \tag{18}$$

and

$$\Delta\bar{\psi} = -\frac{B}{2}\ln\left[\frac{(C'' + \omega x)^2 + y^2}{(C' + \omega x)^2 + y^2}\right] - \frac{A - \omega xB}{y}\left(\operatorname{arctg}\frac{C'' + \omega x}{y} - \operatorname{arctg}\frac{C' + \omega x}{y}\right), \tag{19}$$

where now

$$A = \frac{[(1 - \omega x)^2 + y^2]z_1 - [(1 + \omega x)^2 + y^2]z_2}{2z_1z_2} + \frac{D_1 + D_2}{z_1D_1 - z_2D_2}$$

$$B = \frac{D_2 - D_1}{z_1D_1 - z_2D_2}.$$

We can now put $\Delta\bar{\psi}$ into Eqs. 18 and 19 and evaluate x and y by numerical methods as mentioned above. Substituting these parameters in Eqs. 16 and 17 yields the ion fluxes Φ_1 and Φ_2, and the current density follows again from Eq. 15.[1]

Boundary Conditions

The quantities $\Delta\bar{\psi}$ and $\Delta\bar{P}$ are to be taken inside the membrane, which means that they cannot be measured directly but have to be calculated from data measured in the outer solutions.

We can visualize the membrane boundaries as semipermeable "membranes" being impermeable for the fixed ions of the actual membrane (Schlögl, 1955). According to van't Hoff's law we get the osmotic differerences

$$\bar{P}' = RT \cdot (C'_+ + C'_- - c'_+ - c'_-), \tag{20}$$

$$\bar{P}'' = RT \cdot (C''_+ + C''_- - c''_+ - c''_-) \tag{21}$$

at the boundaries, their difference inside the membrane being

$$\Delta\bar{P} = \bar{P}' - \bar{P}'' = \frac{RTX}{z}\left(C' - C'' - \frac{2zc'}{X} + \frac{2zc''}{X}\right), \tag{22}$$

where $C = z\,(C_+ + C_-)/X$. Assuming Donnan-equilibrium at the boundaries we can write this as

$$\frac{\Delta\bar{P}}{RTX} = \frac{C'}{z} - \frac{C''}{z} - (C'^2 - 1)^{1/2} + (C''^2 - 1)^{1/2}. \tag{23}$$

If we apply a hydrostatic pressure difference P between the two solutions we have

$$\frac{\Delta\bar{P}}{RTX} = \frac{P}{RTX} + \frac{C'}{z} - \frac{C''}{z} - (C'^2 - 1)^{1/2} + (C''^2 - 1)^{1/2}. \tag{24}$$

For measuring the electric potential we use anion reversible electrodes (Ag-AgCl electrodes), which give us the potential difference

$$U = \frac{RT}{Fz_-} \cdot \ln\frac{a'_-}{a''_-} + \frac{RT}{F} \cdot \psi \tag{25}$$

between the metallic components of the electrodes. In addition we get the potential difference

[1]Complex roots are required only for mathematical reasons, as the parameters r and s have no physical meaning. The fact that they may become complex, therefore, has no physical significance.

$$\overline{H} = \frac{RT}{Fz_-} \ln \frac{C''_-}{C'_-} \tag{26}$$

inside the membrane, owing to the concentration gradient. On the assumption that the electrodes are situated directly at the membrane surfaces, i.e., that we do not consider a potential drop in the solutions, the true potential difference inside the membrane is

$$\Delta\overline{\psi} = \frac{F}{RT}(U + \overline{H}). \tag{27}$$

The concentrations C' and C'' are calculated from the Donnan equilibrium at the membrane boundaries. For a symmetric z, $-z$-valent electrolyte they are:

$$C_+ = \left(\frac{X^2}{4z^2} + c^2\right)^{1/2} - \frac{\omega X}{2z}, \tag{28}$$

$$C_- = \left(\frac{X^2}{4z^2} + c^2\right)^{1/2} + \frac{\omega X}{2z}. \tag{29}$$

EXPERIMENTAL METHODS

Apparatus

A cross section of the apparatus used is shown in Fig. 4; it is machined out of one piece of acryl glass. The membrane (exposed area 0.13 cm^2) is sealed with an O-ring on one side and a parafilm gasket on the other side against the membrane holder; in the case of hydrostatic pressures >200 mbar a wide-mesh

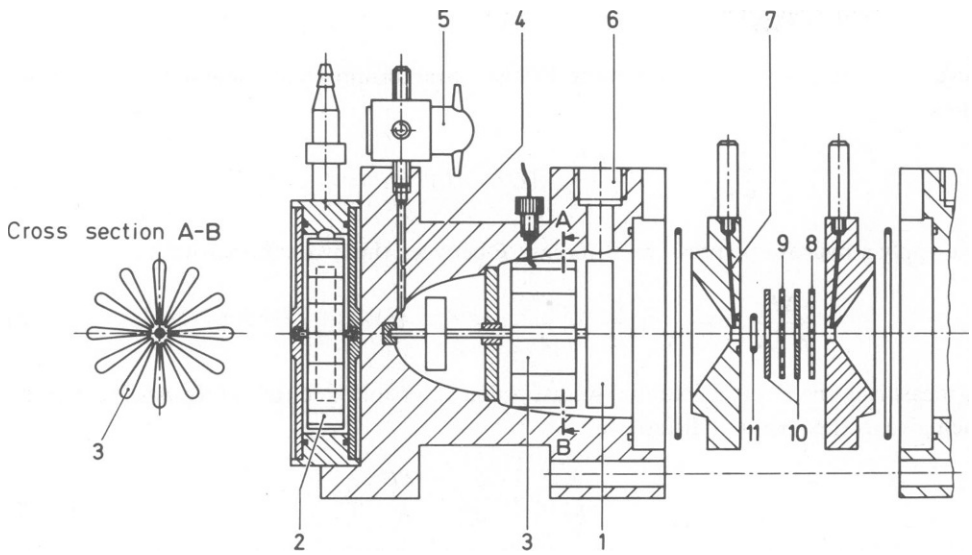

FIGURE 4 Cross-sectional view of half of the cell. stirrer (*1*); vane wheel (*2*); Ag-AgCl electrode (*3*); filling valve (*4*); three-way tap (*5*); outlet suited for connection of a calibrated capillary (*6*); Ag-AgCl electrode (*7*); membrane (*8*); nylon net as a support at high pressure (*9*); parafilm gaskets (*10*); O-ring (*11*).

nylon net is used as a support. One Ag-AgCl electrode close to each surface of the membrane serves for measuring the potential, and one large rosette-shaped Ag-AgCl electrode in the middle portion of each half cell is used to pass an electric current through the membrane. Effective stirring is provided by a blade wheel that is rotated by a stream of water and that via magnetic coupling drives a large paddle inside the cell close to the membrane surface. The half cells can easily be filled free of bubbles because of the particular shape of the compartments. The three-way tap (*5*) can be used to apply a hydrostatic pressure to the cell, and for volume flow measurements a horizontal capillary can be fitted to the outlet (*6*) (calibrated capillaries with divisions of 1 μl were used). The whole cell was kept in a water thermostat at a temperature of 25°C.

The electric circuit contained an electronic potentiostat (G. Bank Elektronik, 34 Göttingen, West Germany), being operated as a galvanostat, which was connected to the large Ag-AgCl electrodes (the current density was always <1 mA/cm^2 electrode area). The current density was displayed on a digital multimeter (Keithley Instruments, Inc., Cleveland, Ohio, model 174) and recorded on an X-Y recorder (Rikadenki Kogyo Co., Ltd., Tokyo, Japan; model RW 101); the membrane potential was measured by a digital electrometer (Keithley model 618, input impedance $2 \cdot 10^{14}$ Ω) and also recorded on the X-Y recorder. The hydrostatic pressure was controlled by a manostat and displayed on a digital manometer (both Wallace & Tiernan Div., Pennwalt Corp., Belleville, N.J.).

The cell was always kept filled and immersed in the thermostat bath to avoid errors caused by swelling of the acryl glass. Before each experiment the solution was thermostated, filled into the cell, and the cell kept again for at least 1 h in the thermostat until measurements were made.

Determination of Membrane Properties

The following procedures were employed to characterize the membranes.

HYDRODYNAMIC PERMEABILITY The cell was filled with the same electrolyte solution in the same concentration on both sides, a hydrostatic pressure difference applied across the membrane and the resulting volume flow per unit time, q, measured by means of a capillary on the low pressure side. The hydrodynamic permeability L_{vv} is then defined as

$$L_{vv} = \frac{q}{A \cdot \Delta P}, \tag{30}$$

where A denotes the membrane area and ΔP the pressure difference.

Except for the membrane CMC, the values of L_{vv} obtained with distilled water and a 0.1 m NaCl solution differed by <5%, and the values obtained at pressures of 0.1 and 3.0 bars differed by <10%.

FIXED ION CONCENTRATION The fixed ion concentration ωX per unit pore volume of the wet membrane was measured by applying a constant voltage across the membrane and measuring the volume flow. From Eq. 14 it follows (with $L_{vv} = d_h/\delta$) that

$$\omega X = \frac{q}{A \cdot L_{vv} \cdot P \cdot \Delta\bar{\phi} \cdot w_v}, \tag{31}$$

where q is the volume flow per unit time, A the membrane area, and $\Delta\bar{\phi} = RT/F \cdot \Delta\bar{\psi}$ the membrane potential according to Eq. 27 when $\overline{H} = 0$. The volume fraction of the pores in the membrane, w_v, has to be taken into account because ωX refers to the pore volume, whereas L_{vv} refers to the total membrane surface.

The results given in Table I were obtained with a 0.1 M NaCl solution on both sides of the membrane, the volume flow being measured in both cell compartments. The measured membrane potential has been corrected for the ohmic potential drop in the solution layers between the electrodes and the membrane surfaces.

VOLUME FRACTION OF THE PORES IN THE MEMBRANE A piece of membrane material is kept in distilled water for 24 h, then it is blotted with filter paper, weighed, and its dimensions are determined. It

is then dried under vacuum at 50°C for 24 h and weighed again. From the difference in weight the volume occupied by water can be determined, and the volume fraction of the pores in the membrane is w_v = volume lost by drying/volume of the wet membrane.

MEMBRANE THICKNESS The thickness of the membrane was determined with a micrometer calliper gauge.

PORE RADIUS Although the membranes used do not have pores of well defined shape and size it is helpful to define an "equivalent pore radius" to characterize their porosities. This equivalent pore radius is the radius of cylindrically shaped pores of an imaginary membrane, having the same hydrodynamic permeability, thickness, and volume fraction of the pores as the membrane to be characterized. Assuming the validity of Hagen-Poiseuille's law for such pores, we can write for the radius

$$a = \left(\frac{8\eta \cdot L_{vv} \cdot \delta}{w_v}\right)^{1/2} \tag{32}$$

where η denotes the viscosity of water, which was taken to be 10^{-9} Js/cm^3. This pore radius is estimated to facilitate comparison between the present data and the literature; it is not used in any of our calculations.

FLIP-FLOP BEHAVIOR OF THE MEMBRANES Galvanostatic voltage-current curves were recorded as described above (see Introduction). The current density was always increased well beyond the point where the volume flow through the membrane reversed (and hence beyond the point where the flip-flop was expected to occur).

All flip-flop experiments were conducted with 0.1 and 0.01 M NaCl solutions, respectively. The data of the membranes described below can be found in Table I.

TABLE I
PROPERTIES OF MEMBRANES USED

Membrane	Membrane material	L_{vv}	ωX	δ	w_v	Equivalent pore radius	Flip-flop behaviour
		(cm⁴/Js)	*(mol/cm³)*	*(μm)*		*(Å)*	
Sartorius SM 11328 (3 layers)	Cellulose nitrate	$5.5 \cdot 10^{-2}$	$-0.8 \cdot 10^{-7}$	270	0.45	510	yes
Sartorius SM 11318 (3 layers)	Cellulose nitrate	$3.5 \cdot 10^{-2}$	$-1.3 \cdot 10^{-7}$	270	0.43	420	yes
Kalle UF PA 20 (3 layers)	Polyamide	$1.2 \cdot 10^{-2}$	$+0.4 \cdot 10^{-7}$	180	0.60	170	yes
S & S El 42	Cellulose nitrate	$3.2 \cdot 10^{-3}$	$-1.0 \cdot 10^{-6}$	160	0.66	80	no
CMC	Carboxy-methyl-cellulose	$4.4 \cdot 10^{-4}$	$-1.8 \cdot 10^{-5}$	120	0.74	20	no
Glass sinter membranes*		15	$-3.0 \cdot 10^{-10}$	650			
Plant cells (*Chara australis, Nitella flexilis*)‡		$1 - 4 \cdot 10^{-4}$	$0.6 \cdot 10^{-3}$	10 (?)			

*Teorell 1959; Franck 1963. The data of the glass sinter and biological membranes are cited for comparison.
‡Dainty and Hope 1959, 1961; Tazawa and Kamiya 1965; Barry and Hope 1969.

RESULTS

Sartorius SM 11328

This cellulose nitrate membrane was used in three layers, pressed onto each other so that no solution could accumulate between them. This increased the potential drop across the membrane and reduced the disturbance caused by stirring in the solutions. (The flip-flops could also be obtained with a single membrane layer, but the recorded curve was extremely unstable at high stirring rates and at high current densities.)

The voltage-current curves obtained with this membrane are depicted in Fig. 5. If the flip- and flop-current densities are approached in small steps, the flip-flops take place in a time of ~1 h (compared with a few seconds in broad pore membranes). The flip- (flop-) transition can be made to occur in ~1 min if the current density is increased (decreased) in a large step beyond the critical value, but then the recorded curve does not represent the true stationary states. The potential measured is the sum of the true membrane potential and the potential drop in the solution between the electrodes and the membrane (this distance was ~0.5 mm), i.e., the true membrane potential is always less than the observed potential.

The theoretical voltage-current curves (which represent potentiostatic measurements) shown in Fig. 6 were calculated with the data given in Table I. (Numerical methods were used to solve the transcendental Eqs. 12, 13, 17, and 18; the calculations were performed on a digital computer PDP 11/20 from Digital Equipment Corp., Maynard, Mass.) The diffusion coefficients of the ions in the membrane were calculated from a formula given by Mackie and Meares (1955):

$$D = D_{aq}\left(\frac{w_v}{2 - w_v}\right)^2, \tag{33}$$

where D_{aq} is the diffusion coefficient of the ions in free solution and w_v is the volume fraction of the pores in the membrane.

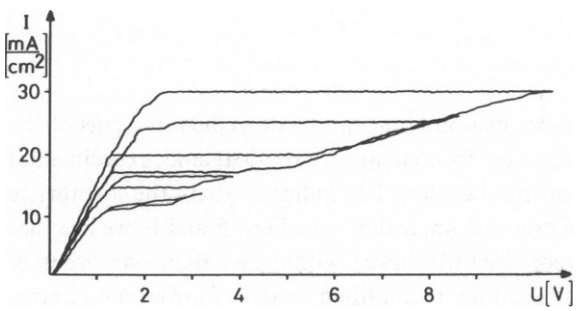

FIGURE 5

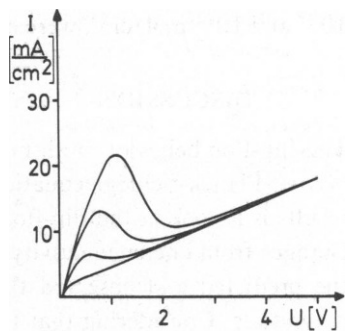

FIGURE 6

FIGURE 5 Galvanostatically recorded voltage-current curves of the Sartorius SM 11328 membrane (three layers). Values of the hydrostatic pressure (starting at the lowest curve): 0, 35, 70, 105 mbar.
FIGURE 6 Theoretical (potentiostatic) voltage-current curves for the SM 11328 membrane (three layers). Values of the hydrostatic pressure (starting at the lowest curve): 0, 35, 70, 105 mbar.

Comparing the flip- and flop currents, we find that the theoretical and experimental results are in close agreement (for a comparison of a galvanostatic and a potentiostatic curve, see Fig. 3).

Sartorius SM 11318

This cellulose nitrate membrane, also used in three layers, behaved very similarly to membrane SM 11328. The flip-flop currents are also in close agreement with the theory.

Kalle UF PA 20

This is a polyamide membrane with a positive fixed ion charge, its hydrodynamic permeability being less than that of the two preceeding membranes. Three layers were used as described above and flip-flops were found in the experiment as well as in the theoretical calculations.

Schleicher and Schüll EI 42

The hydrodynamic permeability of this cellulose nitrate membrane was one order of magnitude lower than that of the Sartorius membranes. Flip-flops neither were found in the experiment (with pressures up to 0.5 bars), nor were they predicted by the theory. Only one layer of this membrane was normally used, but experiments with two or three layers have been performed with no flip-flops.

CMC

No flip-flops were obtained with this membrane (carboxymethylcellulose), whose hydrodynamic permeability was still one order of magnitude less than that of the membrane EI 42, and whose fixed ion concentration was one order of magnitude higher; hydrostatic pressures up to 3.0 bars were used. Again the theory did not predict flip-flops.

Further Membranes

A number of membranes (prepared from carboxymethylcellulose, cellulose acetate), having a hydrodynamic permeability in the order of 10^{-4} cm^4/Js and a fixed ion concentration between 10^{-7} and 10^{-5} mol/cm^3, were also examined, none of which showed flip-flop behavior.

DISCUSSION

The flip-flop behavior of all membranes under examination can be described in terms of the Nernst-Planck-Schlögl equations. The best way to compare theoretical and experimental results is to look at the flip-flop current densities because they indicate where the membrane changes from one conductivity state to the other. Comparing, e.g., Figs. 5 and 6, we see that the predicted and observed flip-flop current densities agree within less than one order of magnitude. Considering that the theory is based on a simplified model of a real membrane, and that certain effects, above all unstirred solution layers, are neglected, it seems justifiable to say that we have a close agreement between theory and experiment. (Kobatake and Fujita [1964*a*, *b*] maintained that the concentration dependence of the electroosmotic coefficient in the equation for the volume flow is a necessary condition for flip-flops to occur and that, e.g., the Nernst-Planck Schlögl equations would not be able to predict such transitions; that this is

in fact not true can be seen from the theoretical results obtained here.) We can, therefore, try to use the theory to obtain information about membranes not investigated experimentally.

The crucial parameters for the occurrence of flip-flops are the hydrodynamic permeability and the fixed ion concentration, because they determine the fluxes through the membrane. Therefore, various combinations of values of these parameters have been assumed in the following computations, once for a membrane thickness of 20 μm and once for 200 μm, keeping the following parameters constant:

$$c' = 0.01 \text{ mol/liter} \qquad c'' = 0.1 \text{ mol/liter}$$

$$D_+ = 1 \cdot 10^{-6} \text{ cm}^2/\text{s} \qquad D_- = 2 \cdot 10^{-6} \text{ cm}^2/\text{s}$$

$$T = 25°\text{C} \qquad P = 0.5 \text{ bars}$$

Numerical methods were again used to evaluate Eqs. 12, 13, 18, and 19. The results are shown in Fig. 7, where the different symbols denote whether a flip-flop occurs for a particular combination of parameters.

In this way we have found a lower limit of the hydrodynamic permeability and an upper limit of the fixed ion concentration beyond which a membrane will show no flip-flop behavior; this agrees with our experimental results.

To illustrate in which way these limits depend on the other parameters, the computations were repeated for a pressure of 5 bars. The results are similar to those shown in Fig. 7, except that the region in which flip-flops were found extends down to $L_{vv} \simeq 2 \cdot 10^{-3}$ cm^4/Js and up to $\omega X \simeq 2 \cdot 10^{-5}$ mol/cm^3 for a membrane of 200 μm thickness. On the assumption that the diffusion coefficients are $D_+ = 1 \cdot 10^{-7}$ cm^2/s and $D_- = 1 \cdot 10^{-5}$ cm^2/s, the theory yields flip-flops down to $L_{vv} \simeq 5 \cdot 10^{-4}$ cm^4/Js and up to $\omega X \simeq 10^{-4}$ mol/cm^3 (for a membrane

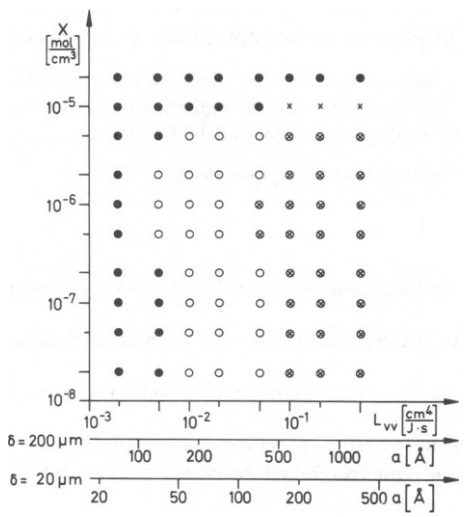

FIGURE 7 Flip-flops predicted by the theory for various combinations of parameters (as explained in the text): ●, no flip-flop predicted; ○, flip-flop predicted for a membrane thickness of 200 μm; ×, flip-flop predicted for a membrane thickness of 20 μm.

thickness of 200 μm and a pressure of 0.5 bars). Increasing the concentration ratio c''/c' has a similar effect.

So far we have shown that synthetic membranes are able to produce stationary state flip-flops only if their fixed ion concentration is below and their hydrodynamic permeability is above critical values which depend on other system parameters, as outlined above.

Let us now turn to the Teorell oscillator as a possible analogue of biological excitable systems. Here we have in mind certain plant cells for which there is clearly a hydrostatic pressure difference across the excitable membrane. We shall specifically deal with one example, where sufficient data are available: The internodal cells of the algae *Chara australis*.

The "wall" of such a cell consists of several layers: tonoplast, cytoplasm, plasmalemma, and cell wall (Mailman and Mullins, 1966). The following data are available: $\omega X \simeq 6 \cdot 10^{-4}$ mol/cm^3 (located in the cell wall; Dainty and Hope, 1959*b*); $L_{vv} \simeq 1 - 3 \cdot 10^{-4}$ cm^4/Ms (measured between inside and outside; Dainty and Hope, 1959*a*); $\delta \simeq 20$ μm (cell wall plus plasmalemma plus cytoplasm; Mailman and Mullins, 1966).

We shall now simplify our considerations by regarding the series array of tonoplast, cytoplasm, plasmalemma, and cell wall as one membrane having the above properties. Thus, we can locate this sytem in Fig. 7. Even if we consider that the hydrostatic pressure difference is 6–8 atm (Barry, 1970), we have to conclude that the theory would not predict flip-flops.

Of course our comparison can only be understood as a very crude test. It shows clearly, however, which orders of magnitude certain parameters of a biological membrane have to assume if the Teorell oscillator mechanism is to be relevant for this membrane. It is not very likely to be the source of excitability in the example given above, and consequently the same is also true of many other plant cells. On the other hand, the membrane properties for which the theory predicts flip-flops cannot be regarded as being biologically unreasonable. Therefore we do not think that it can be excluded that the Teorell mechanism works somewhere in biological systems, even if at present we are not aware of any particular one.

We are very grateful to Prof. R. Schlögl, Max-Planck-Institut für Biophysik, Frankfurt, and to Prof. P. Meares, Aberdeen University, for helpful discussions and valuable suggestions. Furthermore, we thank Mr. R. Gröpl for the preparation of membranes and Mr. R. Bomsdorf for machining the cell.

Received for publication 23 July 1980 and in revised form 10 April 1981.

REFERENCES

Barry, P. H., and A. B. Hope. 1969. Electroosmosis in membranes: effects of unstirred layers and transport numbers. *Biophys. J.* 9:729–757.

Barry, P. H. 1970. Volume flows and pressure changes during an action potential in cells of *Chara australis*. *J. Membr. Biol.* 3:313–334.

Dainty, J., and A. B. Hope. 1959*a*. The Water permeability of cells of *Chara australis R. Br. Aust. J. Biol. Sci.* 12:136–145.

Dainty, J. and A. B. Hope. 1959*b*. Ionic relations of cells of *Chara australis*. *Aust. J. Biol. Sci.* 12:395–411.

Drouin, H. 1969*a*. Experimente mit dem Teorellschen Membranoszillator. *Ber. Bunsen-Ges. Phys. Chem.* 73:223–229.

Drouin, H. 1969*b*. Über nichtlineare Elektroosmose. *Ber. Bunsen-Ges. Phys. Chem.* 73:590–596.

Franck, U. F. 1963. Über das elektrochemische Verhalten von porösen Ionenaustauschermembranen. *Ber. Bunsen-Ges. Phys. Chem.* 67:657–671.

Franck, U. F. 1967. Phänomene an biologischen und künstlichen Membranen. *Ber. Bunsen-Ges. Phys. Chem.* 71:789–799.

Kobatake, Y., and H. Fujita. 1964*a*. Flows through charged membranes. I. Flip-flop current vs. voltage relation. *J. Chem. Phys.* 40:2212–2218.

Kobatake, Y., and H. Fujita. 1964*b*. Flows through charged membranes. II. Oscillation phenomena. *J. Chem. Phys.* 40:2219–2222.

Mackie, J. S., and P. Meares. 1955. The diffusion of electrolytes in a cation exchange resin membrane. *Proc. R. Soc. Lond. A Math. Phys Sci.* 232:498–509.

Mailman, D. S., and L. J. Mullins. 1966. The Electrical measurement of chloride fluxes in *Nitella*. *Aust. J. Biol. Sci.* 19:385–398.

Meares, P. and K. R. Page. 1972. Rapid force-flux transitions in highly porous membranes. *Philos. Trans. R. Soc. Lond. A Math. Phys. Sci.* 272:1–46.

Meares, P. and K. R. Page. 1973. The Teorell Oscillator as a mechanoelectric transducer. *J. Membr. Biol.* 11:197–216.

Meares, P. and K. R. Page. 1974. Oscillatory fluxes in highly porous membranes. *Proc. R. Soc. Lond. A Math. Phys. Sci.* 339:513–532.

Page, K. R. and P. Meares. 1974. Factors controlling the frequency and amplitude of the Teorell oscillator. *Faraday Symp. Chem. Soc. Lond.* 9:166–173.

Schlögl, R. 1955. Zur Theorie der anomalen Osmose. *Z. Phys. Chem.* N. F. 3:73–102.

Schlögl, R. and U. Schödel. 1956. Über das Verhalten geladener Porenmembranen bei Stromdurchgang. *Z. Phys. Chem.* N. F. 5:372–397.

Schlögl, R. 1966. Membrane permeation in systems far from equilibrium. *Ber. Bunsen-Ges. Phys. Chem.* 70:400–414.

Schmid, G. 1950. Zur Elektrochemie feinporiger Kapillarsysteme. I. Übersicht. *Z. Elektrochem.* 54:424–430.

Schmid, G. 1951. Zur Elektrochemie feinporiger Kapillarsysteme. II. Elektroosmose. *Z. Elektrochem.* 55:229–237.

Schmid, G. 1952. Zur Elektrochemie feinporiger Kapillarsysteme. VI. Konvektionsleitfähigkeit (theoretische Betrachtung). *Z. Elektrochem.* 56:181–193.

Schmid, G. and H. Schwarz. 1951. Zur Elektrochemie feinporiger Kapillarsysteme. III. Elektrische Leitfähigkeit. *Z. Elektrochem.* 55:295–307.

Schmid, G. and H. Schwarz. 1952. Zur Elektrochemie feinporiger Kapillarsysteme. V. Strömungspotentiale; Donnan-Behinderung des Elektrolytdurchgangs bei Strömungen. *Z. Elektrochem.* 56:35–44.

Tazawa, M. and Kamiya, N. 1965. Water relations of *Chara* internodal Cell. *Annu. Rep. Biol. Works. Fac. Sci. Osaka Univ.* 13:123–130.

Teorell, T. 1956. Transport phenomena in membranes. *Disc. Faraday Soc.* 21:9–26.

Teorell, T. 1958. Rectification in a plant cell (*Nitella*) in relation to electro-endosmosis. *Z. Phys. Chem.* N. F. 15:385–398.

Teorell, T. 1959*a*. Elektrokinetic membrane processes in relation to properties of excitable tissues. I. Experiments on oscillatory transport phenomena in artificial membranes. *J. Gen. Physiol.* 42:831–846.

Teorell, T. 1956*b*. Elektrokinetic membrane processes in relation to properties of excitable tissues. II. Some theoretical considerations. *J. Gen. Physiol.* 42:847–863.

Teorell, T. 1961*a*. Oscillatory electrophoresis in ion exchange membranes. *Ark. Kemi* 18:401–408.

Teorell, T. 1961*b*. An analysis of the current-voltage relationship in excitable *Nitella* cells. *Acta Physiol. Scand.* 53:1–6.